PAPER

Laponite®-based colloidal nanocomposites prepared by RAFT-mediated surfactant-free emulsion polymerization: the role of non-ionic and anionic macroRAFT polymers in stability and morphology control†

Thaíssa C. Chaparro, [ID] ‡[a,b] Rodrigo D. Silva, [ID] §[b] Pierre-Yves Dugas,[a] Franck D'Agosto, [ID] [a] Muriel Lansalot, [ID] [a] Amilton Martins dos Santos [ID] *[b] and Elodie Bourgeat-Lami [ID] *[a]

The synthesis of Laponite®-based composite latexes by reversible addition-fragmentation chain transfer (RAFT)-mediated surfactant-free emulsion polymerization is described. RAFT homopolymers and copolymers (macroRAFT agents) comprising acrylic acid (AA), poly(ethylene glycol) (PEG) segments and *n*-butyl acrylate (BA) repeating units were adsorbed onto exfoliated Laponite® in aqueous dispersion, and subsequently chain extended by methyl methacrylate and BA to form colloidal nanocomposites. The high hydrophilicity of PAA macroRAFT agents led to unstable latexes as polymerization took place mainly in the aqueous phase. Differently, PEG-based RAFT copolymers adsorbed more strongly onto Laponite® and favored morphology control. The free macroRAFT chains engaged preferably in the stabilization of the hybrid structures, rather than in the formation of free latex particles, resulting primarily in a Janus morphology. The presence of BA units in the macroRAFT structure helped further in confining the polymerization on the clay surface and enabled the morphology of the particles to be tuned resulting in the formation of dumbbell or sandwich-like structures. These results show that the parameters driving the competing mechanisms related to the polymerization locus, such as the presence of free macroRAFTs, the affinity between macroRAFTs and clay and the adequate hydrophilic–hydrophobic balance within the macroRAFT structure, are key for assuring both the stabilization of the nanocomposite particles and the control of their morphology.

1. Introduction

In recent years, waterborne processes have emerged as versatile techniques for the production of nanocomposites and for tailoring their properties.[1] Among the various inorganic particles, clay minerals have attracted considerable attention. Indeed, the incorporation of layered silicates into nanocomposites,

[a]Univ Lyon, University Claude Bernard Lyon 1, CPE Lyon, CNRS, UMR 5265, Chemistry, Catalysis, Polymers and Processes (C2P2), 43, Blvd du 11 Novembre 1918, F-69616 Villeurbanne, France. E-mail: Elodie.BOURGEAT-LAMI@univ-lyon1.fr
[b]Engineering School of Lorena – University of São Paulo, 12.602-810 Lorena, SP, Brazil
†Electronic supplementary information (ESI) available. See DOI: 10.1039/d0py00720j
‡Current address: Univ. Bordeaux, CNRS, Bordeaux INP, LCPO, UMR 5629, F-33600, Pessac, France.
§Current address: Centro Universitário de Formiga, 328 Doutor Arnaldo de Senna Ave., 35574-570 Formiga/MG, Brazil.

even at very low levels, can provide various advantages to the resulting hybrid materials, when compared to pure polymers. Moreover, having polymer/layered silicate nanocomposite particles in the form of a colloidal dispersion in a continuous aqueous medium can confer very practical and interesting applications to these materials. First and foremost, the use of water as a dispersion medium allows adequate conditions for the exfoliation of the silicate platelets.[2] In addition, the composite suspension can be easily handled and, when film-forming materials are used, hybrid latexes can be further processed into films with outstanding properties.[3,4]

In this respect, controlling the morphology of the hybrid particles is of major importance for many applications. Polymer/inorganic Janus particles, for example, can be an interesting alternative to stabilize emulsions or as building blocks of complex self-assembled structures. Furthermore, the formation of core–shell particles by encapsulation techniques, for instance, can be an ultimate goal to form homogeneous

nanostructured films and ensure that inorganic objects remain separated during the film formation process.

Among the different methods to prepare nanocomposite particles in aqueous dispersed media, the use of reversible addition-fragmentation chain transfer (RAFT) polymerization has proved to be an effective technique to tailor particle morphology. In a process coined RAFT-assisted encapsulating emulsion polymerization (REEP), macromolecular RAFT (macroRAFT) agents are used to direct (and preferably restrict) the growth of the polymer chains to the surface of the inorganic particles.[5] This process takes advantage of the developments in the polymerization-induced self-assembly (PISA) technique, in which water-soluble RAFT copolymers are chain extended in water with hydrophobic monomers, resulting in the *in situ* formation of self-assembled diblock copolymer particles of different morphologies. In the REEP strategy, the adsorbed macroRAFTs also provide reactivatable sites from which chain extension can proceed to generate an insoluble segment at the inorganic particle surface, self-stabilized by the hydrophilic block in a cooperative co-assembly process involving free and adsorbed copolymers, thus discarding the need for an additional surfactant.[6,7] The REEP strategy has been used to synthesize composite latexes incorporating diverse spherical inorganic particles, including alumina and zirconia-coated titanium dioxide pigments,[5] different metal, metal oxide and metal nitride particles,[8] cadmium sulfide[9] and lead sulfide[10] quantum dots, cerium oxide,[11–14] iron oxide[15] and silica.[16] Two-dimensional (2D) inorganic particles (*i.e.* sheets or platelets) have also been investigated.[17–22]

In the pioneering work of Ali and co-workers,[17] amphipathic trithiocarbonate macroRAFT agents composed of acrylic acid (AA) and *n*-butyl acrylate (BA) units were used to encapsulate gibbsite platelets with a P(MMA-*co*-BA) layer. The composition of the random RAFT copolymers was shown to be key in locating the polymerization at the inorganic surface and promoting encapsulation. In addition, a random composition was selected to prevent the macroRAFT from self-assembling into micelles, limiting the formation of pure polymeric particles in the water phase by secondary nucleation. Yet, stability issues arose when relatively more hydrophilic copolymers were employed, as they were less inclined to adsorb on the growing nanocomposite particles during polymerization to sustain colloidal stability, causing consequently their aggregation. Since then, other anisotropic particles such as graphene oxide (GO),[18] layered double hydroxides (LDHs)[19,20] and montmorillonite (MMT)[21,22] have been the object of study of this strategy. In the presence of LDH nanoparticles, the use of statistical copolymers of AA and BA has resulted in encapsulated or, depending on the molar mass of the RAFT copolymer, sandwich particle morphologies. Interestingly, when the RAFT function was removed from the macroRAFT agents, armored composite particles were produced, emphasizing the importance of the living character of the macroRAFT copolymer (*i.e.* its ability to provide reactivatable sites from which chain extension can proceed) in promoting the formation of an even polymer coating around the inorganic nanoparticles and

achieving kinetically trapped morphologies. In the case of MMT, cationic random RAFT copolymers composed of quaternized dimethylaminoethyl acrylate (DMAEA) and BA have been used to adsorb on the clay by electrostatic interaction and stabilize the hybrid latexes, resulting in the formation of "cornflake"-like particles.[21] In another work with MMT, Silva *et al.*[22] showed that the use of anionic macroRAFT copolymers led to polymer-decorated clay platelets, while the concomitant use of a non-ionic and an anionic macroRAFT agent led to a higher polymer coverage of the clay platelets. Full encapsulation was achieved with 2-dimethylaminoethyl methacrylate (DMAEMA)-based macroRAFT agents, which interacted more strongly with the clay surface. Particularly, the use of a RAFT terpolymer composed of DMAEMA, BA and poly(ethylene glycol) methyl ether acrylate (PEGA) led to uniform encapsulation and minimization of free polymer particle formation in the water phase.

For Laponite®, to the best of our knowledge, only one work involving a linear PEG-terminated RAFT agent has reported the use of RAFT polymers to produce hybrid particles by the REEP method.[23] Adsorption of the PEG macroRAFT onto Laponite® was key to prevent its partition between the water and monomer phases, and guarantee the control of the polymerization and good colloidal stability. The nanocomposite latex showed an armored morphology as a result of co-assembly and/or heterocoagulation events between chain extended macroRAFT agent-adsorbed clay platelets and block copolymer nano-objects formed in the water phase by PISA. Such a morphology can be advantageous not only for the colloidal stability of the system but also for the mechanical properties of the film, as it results in honeycomb structures. Yet, the armored morphology was observed only under specific conditions, and a deeper study on the use of the REEP technique, using Laponite® and macroRAFT agents with different structures and compositions, under various reaction conditions, still needs to be carried out in order to further explore and understand the parameters influencing the stability and the morphology of the final composite particles.

This work reports the use and evaluation of the REEP strategy to control the morphology of P(MMA-*co*-BA)/Laponite® nanocomposite latex particles using different macroRAFT agent structures. It follows a previous study in which RAFT copolymers have been designed and synthesized by solution polymerization and evaluated in an adsorption study onto Laponite®.[24] In the present work, emulsion copolymerization of MMA with BA was performed in the presence of Laponite® platelets modified with AA-, PEG- or PEGA- and BA-based macroRAFT copolymers to generate clay/polymer nanocomposite latex particles under semi-batch surfactant-free conditions.

2. Experimental section

2.1. Materials

MacroRAFT agents with different hydrophilic–lipophilic balances were used in this work, as listed in Table 1. They were

Table 1 Structure, molar mass of each macroRAFT agent (determined using the individual monomer conversion obtained by ^{1}H NMR analysis), experimental molar mass (obtained by SEC) and dispersity of macroRAFT agents used in this work, and their adsorbed amount at saturation (q_{max}) according to the Langmuir model[24]

Entry	MacroRAFT	$M_{n, NMR}$ (g mol^{-1})	$M_{n, SEC}$ (g mol^{-1})	$Đ$	q_{max} (mg g^{-1})
M1	PAA$_{40}$-TTC	3120	3630	1.19	18
M2	PEG$_{45}$-b-PAA$_{42}$-TTC	5310	6710	1.18	173
M3^a	PAA$_{40}$-b-PPEGA$_4$-TTC	5460	4640	1.31	453
M4^a	PAA$_{40}$-b-P(PEGA$_6$-co-BA$_4$)-TTC	7230	6130	1.21	488
M5^a	P(PEGA$_6$-co-BA$_4$)-TTC	3040	2900	1.12	466
M6	P(AA$_{16}$-co-BA$_{16}$)-TTC	3440	3420	1.26	320

^{a} PEGA M_n = 480 g mol^{-1}; PPEGA = poly(poly(ethylene glycol) methyl ether acrylate).

synthesized using 4-cyano-4-thiothiopropylsulfanyl pentanoic acid (TTC) as the RAFT agent and purified as described previously.[24] Their synthesis followed a controlled behavior as indicated by a linear evolution of molar mass with time and low dispersities ($Đ = M_w/M_n$), ensuring that they could be further chain extended. Laponite® RD (BYK Additives Ltd) was used as the clay component. Laponite® was chosen among the layered silicates, since it is an ideal model substrate, presenting a high chemical purity, a uniform dispersity of the elementary platelets, disposed in the form of disc-shaped crystals with a diameter of ~25–30 nm and a thickness of ~0.92 nm, and the ability to produce clear dispersions. Tetrasodium pyrophosphate (95%, Aldrich) was added to Laponite® powder for polymerizations carried out using the non-ionic macroRAFT agent M5, to hinder gel formation and avoid the formation of "house of cards" structures.[25,26] Laponite® RD (without adding a peptizer) was used in all other cases in order to allow interaction with the clay edges.

Sodium hydroxide (NaOH 1 N, standard, Acros Organics) and the initiator 4,4′-azobis(cyanopentanoic acid) (ACPA, ≥98%, Sigma-Aldrich) were used as received. The monomers: methyl methacrylate (MMA, 99%, Sigma-Aldrich) and n-butyl acrylate (BA, 99%, Sigma-Aldrich) were used without further purification.

2.2. Methods

Laponite®/polymer hybrid latexes were synthesized in the presence of macroRAFT agents using a semi-continuous process. In a typical run (R4B as an example), 0.125 g of Laponite® were added to a flask containing 10 mL of water. In the specific case of M5, a peptizing agent was added to the clay (10 wt%). The dispersion was left under vigorous stirring for 30 minutes while, in parallel, the required amount of the macroRAFT agent (final concentration of macroRAFT = 2.2 mM) was added to a flask with 10 mL of water and the pH was adjusted with NaOH solution (for the experiments carried out at low pH values, there was no need to adjust the pH with acidic solution as the resulting dispersion was acidic). The Laponite® dispersion was added to the flask containing the macroRAFT solution. The Laponite®/macroRAFT suspension was left stirring for 60 minutes and transferred to a 50 mL three-neck round-bottom flask, where 0.1 g of the monomer mixture (MMA/BA

Table 2 Typical recipe and conditions used in the synthesis of hybrid latexes by RAFT-mediated surfactant-free emulsion polymerization in the presence of macroRAFT agents^a

[Laponite®] (g L^{-1})	5
[MacroRAFT]/[initiator] (mol/mol)	3
Monomer initial shot (mL)	0.1
Monomer added (mL)	2.4
Monomer addition rate (mL h^{-1})	0.6
Total volume (mL)	25
Temperature (°C)	80

^{a} [MacroRAFT] = 2.2 mM.

containing 80 wt% of MMA) and 2.6 mL of a solution of the initiator previously prepared (at a molar concentration 3 times lower than that of macroRAFT and containing ~15 μL of a 1 N NaOH solution) were added. The system was adapted to a reflux condenser, a stirring plate and purged with nitrogen for 30 minutes, while the monomer mixture was purged in a separate flask. To start polymerization, the system was heated to 80 °C, and 2.4 mL of the monomer mixture were fed at 0.6 mL h^{-1} for 4 hours. Polymerization was left for additional 2 hours after the end of the monomer addition and samples were taken every hour for kinetics study. A typical recipe and conditions used in the synthesis are shown in Table 2.

2.3. Characterization

Monomer conversions were determined by gravimetric analysis. The average hydrodynamic particle diameter ($Z_{av.}$) was determined by dynamic light scattering (DLS) in a Zetasizer Nano ZS instrument from Malvern. The broadness of the distribution was given by a dimensionless number called PdI, determined from the autocorrelation function using the second-order method of cumulant analysis. The higher this value, the broader the size distribution. Although DLS is more indicated for spherical particles and does not provide an exact $Z_{av.}$ value for disc- or dumbbell-shaped objects (such as Laponite® platelets and some of the hybrid particles observed in this work), it can be considered as a useful tool for comparing the samples. Particle morphology was determined by cryogenic transmission electron microscopy (cryo-TEM) using a Philips CM120 transmission electron micro-

scope from the Centre Technologique des Microstructures (CTμ), platform of the Université Claude Bernard Lyon 1, in Villeurbanne, France. A drop of the dilute suspension was deposited on a holey carbon-coated copper grid and, before introduction in the microscope, the excess of liquid was removed from the grid using filter paper. The grid was then immersed in a liquid ethane bath cooled with liquid nitrogen and positioned on the cryo-transfer holder, which kept the sample at −180 °C and guaranteed a low-temperature transfer to the microscope. The images of the frozen hydrated latex specimens were acquired at an accelerating voltage of 120 kV. In the case of the formation of spherical particles, the number and weight average particle diameters (D_n and D_w, respectively) and the polydispersity index (D_w/D_n) were calculated using $D_n = \sum n_i D_i / \sum n_i$ and $D_w = \sum n_i D_i^4 / \sum n_i D_i^3$, where n_i is the number of particles with diameter D_i. At least 200 particles were counted for each batch.

For the estimation of the fraction of secondary nucleated polymer latex particles, the average volume of each nodule ($V_{nodules}$, nm^3) was first obtained considering that the nodules are spherical, according to eqn (1):

$$V_{nodules} = \frac{4}{3} \times \pi \times \left(\frac{D_{nodule}}{2}\right)^3 \quad (1)$$

where D_{nodule} is the diameter of the nodules determined by cryo-TEM (D_n, nm).

The total number of polymer nodules per liter of reaction mass ($N_{nodules}$ per L) was then calculated according to eqn (2), considering that PC is the polymer content (g L^{-1}) and ρ_{pol} is the density of the polymer (all samples were considered to have the average density of P(MMA-co-BA), 1.16 g cm^{-3}):

$$N_{nodules} \, \text{per L} = \frac{PC}{V_{nodules} \times \rho_{pol}} \times 10^{21} \quad (2)$$

The number of Laponite® platelets per liter of reaction ($N_{Laponite®}$ per L) was estimated according to eqn (3):

$$N_{Laponite®} \, \text{per L} = \frac{[\text{Laponite®}]}{\pi \times \left(\frac{d}{2}\right)^2 \times h \times \rho_{Lap}} \times 10^{21} \quad (3)$$

where [Laponite®] is the mass concentration of Laponite® added in the formulation of the latex (g L^{-1}), d is the average diameter (d = 25 nm), h is the average thickness (h = 0.92 nm) of the platelets and ρ_{Lap} is the density of Laponite® (ρ_{Lap} = 2.53 g cm^{-3}).[35]

The fraction of Laponite®-free nodules ($P_{free nodules}$), assuming no free clay platelets and that all composite particles have a Janus morphology (*i.e.*, there are as many composite nodules as clay platelets since each clay sheet is associated with a single polymer nodule, *vide infra*), was then estimated according to eqn (4):

$$P_{free nodules}(\%) = \frac{(N_{nodules} - N_{Laponite®})}{N_{nodules}} \times 100 \quad (4)$$

3. Results and discussion

In this work, amphipathic macroRAFT agents, carrying a reactivatable thiocarbonylthio functionality and suitable anchor groups, have been carefully designed to interact with Laponite® particles, control the subsequent radical copolymerization of MMA with BA and stabilize the growing hybrid particles. The synthesis of these living macromolecules and their ability to interact with the Laponite® surface have already been shown in a previous study,[24] which is used as the basis for the present work. The focus now is to evaluate the capacity of these macromolecules to control the stability and morphology of nanocomposite latexes containing Laponite® platelets *via* the REEP method.

As listed in Table 1, the designed macromolecules contain AA, PEG (linear or comb-like) and BA units, combined in various ways. Reinitiation and propagation of the hydrophobic block can occur from either the anionic (for M1, M2 and M6) or the non-ionic (M3, M4 and M5) block. As shown in our previous work,[24] each macroRAFT chosen can interact with Laponite® *via* different adsorption mechanisms. PEG is known to strongly adsorb on the basal surface of the clay particles. PAA could be expected to adsorb on the positively charged rims of the clay; however, it has been shown that at pH 7.5, charge repulsion between PAA and the negatively charged surface of Laponite® predominates over attractive interactions, prejudicing adsorption. The incorporation of ethylene glycol units in the copolymers has a notable effect on the adsorption process when compared to pure PAA, being more favorable when PEG is disposed as pendent segments, rather than in a linear configuration. Furthermore, hydrophobic BA moieties have been shown to favor adsorption.

Hybrid latexes were prepared by surfactant-free starve-feed emulsion polymerization in the presence of the macroRAFT and clay particles. Besides the nature of the macroRAFT agent, some other parameters were evaluated in this work, including the pH and monomer composition. The results, in terms of final conversion, hydrodynamic particle diameter ($Z_{av.}$) and size dispersity, are listed in Table 3.

3.1. Hybrid latexes synthesized with PAA$_{40}$ (M1)

The first investigated macroRAFT agent was PAA$_{40}$-TTC (M1, Table 1). This hydrophilic homopolymer is not expected to form micelles and is pH dependent. Considering that the pK_a of PAA is ~6,[27,28] this macroRAFT is expected to be predominantly deprotonated and consequently negatively charged above pH 6. For this reason, three different pH values were tested in R1A, R1B and R1C: pH = 5.0, 7.5 and 12, corresponding, respectively, to the acidic, neutral and alkaline conditions.

Overall and instantaneous conversions *versus* time curves are shown in the ESI, Fig. S1.† Final latexes had poor colloidal stability for all the pH values tested, which was indicated by the sedimentation of particles during polymerization, even though this is not evidenced by the data corresponding to pH 5 and 12 in Fig. S1.† Indeed, the presence of large aggregated

Table 3 Experimental conditions and characteristics of Laponite®/P(MMA-co-BA) hybrid latexes synthesized by RAFT-mediated surfactant-free emulsion polymerization using anionic (M1, M2, M3, M4 and M6) and non-ionic (M5) macroRAFT agents[a]

Exp.	MacroRAFT	MMA/BA (wt/wt)	pH	[Laponite®] (g L^{-1})	Conversion (%)	$Z_{av.}$/PdI (nm)
R1A	M1	80/20	5.0	5	65	Unstable
R1B	M1	80/20	7.5	5	63	Unstable
R1C	M1	80/20	12.0	5	68	Unstable
R2A	M2	80/20	4.5	5	63	Unstable
R2B	M2	80/20	7.5	5	96	185/0.17
R2C	M2	80/20	12.0	5	78	130/0.06
R3A	M3	80/20	3.0	5	66	131/0.63
R3B	M3	80/20	7.5	5	98	76/0.09
R3C	M3	80/20	12.0	5	86	116/0.10
R4A	M4	80/20	5.0	5	72	53/0.16
R4B	M4	80/20	7.5	5	94	56/0.14
R4C	M4	80/20	12.0	5	79	82/0.09
R4D	M4	90/10	7.5	5	89	46/0.15
R4E	M4	100/0	7.5	5	97	58/0.06
R5A	M5	90/10	10.0	5	78	Unstable
R5B[b]	M5	90/10	10.0	5	79	132/0.22
R5C	M5	90/10	10.0	0	68	Unstable
R6	M6	90/10	7.5	5	82	70/0.17

[a] M1 = PAA$_{40}$-TTC; M2 = PEG$_{45}$-b-PAA$_{42}$-TTC; M3 = PAA$_{40}$-b-PPEGA$_4$-TTC; M4 = PAA$_{40}$-b-P(PEGA$_6$-co-BA$_4$)-TTC; M5 = P(PEGA$_6$-co-BA$_4$)-TTC; and M6 = P(AA$_{16}$-co-BA$_{16}$)-TTC. [b] Sonication for 5 minutes prior to polymerization.

particles during polymerization could be observed in all cases, and might have prejudiced the withdrawal of samples, giving unreliable conversions and $Z_{av.}$ values.

The adsorption isotherm of PAA-TTC at pH 7.5 revealed a weak macroRAFT/clay interaction.[24] Such low affinity was attributed to charge repulsion between the anionic macroRAFT and the clay surface. Indeed, spillover of the negative electrical potential from the particle faces into the edge region resulted in a negative potential everywhere around the particles, preventing PAA adsorption on the positive clay edges. As a consequence, only 1 mol% of the added macroRAFT is adsorbed on the surface of Laponite® at the beginning of polymerization under the experimental conditions used in this work. Therefore, the mechanisms of particle formation and, consequently, the stability problem, are likely related to important secondary nucleation and events taking place in water. In the emulsion polymerization mediated by hydrophilic macroRAFT agents, nucleation is expected to occur according to the PISA mechanism, resulting in amphiphilic block copolymers that self-assemble and produce self-stabilized latex particles. In the absence of clay, it has already been shown in the literature[29] that chain extension of PAA with styrene proceeds according to the PISA mechanism under acidic conditions (pH = 2.5). At higher pH values, however, the ionization of AA affects the nucleation process, by interfering in the reinitiation of PAA during the first addition-fragmentation steps, and only a fraction of the PAA chains effectively reinitiated the polymerization of styrene still giving rise to a stable latex. When clay platelets are present, a small part of the macroRAFT agent is adsorbed on the inorganic surface (around 1 mol% at pH 7.5, but likely pH-dependent) and this should lead to competing events in water with nucleation and stabilization processes taking place not only in the continuous phase but also on the clay platelets. However, the

formation of aggregates since the early stages of polymerization, independently of the pH (and thus of the quality of the control), indicates that the presence of platelets might have a greater than predicted effect on particle nucleation. Some examples in the literature that used PAA-TTC to synthesize hybrid particles in the presence of different inorganic nano-objects also reported stability issues.[5,9,11] In these cases, instability was related to secondary nucleation associated with the ability of this highly hydrophilic macroRAFT agent to desorb rather easily from the inorganic surface. So the newly formed particles competed with the inorganics for stabilizing macroRAFT chains and, as the amount of macroRAFT molecules was not enough to stabilize all created interfaces, colloidal stability was not achieved.

3.2. Hybrid latexes synthesized with PEG$_{45}$-b-PAA$_{42}$ (M2)

The high affinity between PEG and clays is well known.[30] Indeed, a strong adsorption of PEG chains onto Laponite® platelets has already been reported in the literature.[23,24] So, to encourage the approach of the PAA block to the basal faces of the platelets, PAA was combined with a PEG chain and the resulting PEG$_{45}$-b-PAA$_{42}$-TTC block copolymer was evaluated in the synthesis of hybrid latexes (M2, Table 1). The great feature of this double-hydrophilic block copolymer is that while the PEG block interacts with Laponite® and screens the clay surface charges promoting the approach of the highly hydrophilic PAA segment to the inorganic particle, some carboxylate groups (for pH values higher than the pK_a of PAA) are free in the aqueous phase surrounding the platelets, generating a double effect of stabilization (electrosteric). According to the adsorption isotherm of this macroRAFT agent,[24] at the concentration of macroRAFT used in the synthesis, around 6 mol% of the macroRAFT chains are adsorbed on the surface of

Laponite® at pH 7.5, while the remaining chains are free in water.

At low pH, however, hydrogen bonds can be formed between the ether units of PEG and the carboxyl groups of PAA, resulting in water-insoluble intramolecular complexes.[31–34] In our case, one of the pH values tested (4.5) approaches the pH of complexation and, therefore, stability issues could be expected in this case. Indeed, the latex obtained at pH 4.5 (R2A in Table 3) presented no colloidal stability, but at higher pH values (pH = 7.5, R2B and pH = 12, R2C), final latexes with higher stability and monomer conversions were obtained, as shown in Fig. S2.†

The pH of the medium affects the polymerization kinetics, as shown in Fig. S2 of the ESI.† While 93% conversion was obtained at pH 7.5, a limiting final conversion of 63% was obtained at pH = 4.5 likely due to the poor colloidal stability of this latex. In addition, although the samples were stable in that case, considerably large final particles were obtained at pH 7.5 and 12 (185 and 130 nm, respectively). Indeed, the configuration of the molecule, with the TTC group located at the end of the PAA segment, as schematically shown in Fig. 1, may be another drawback of this copolymer. Such configuration can force the growing hydrophobic block to assume an inconvenient location, by leaving the hydrophilic AA segment buried inside the polymer shell as a loop, which may not be enough for stabilization purposes.

3.3. Hybrid latexes synthesized with PAA$_{40}$-b-PPEGA$_4$ (M3)

To avoid both drawbacks (*i.e.*, the formation of intramolecular complexes and the burial of PAA during hydrophobic chain growth), we next evaluated the PAA$_{40}$-b-PPEGA$_4$-TTC macroRAFT (M3, Table 1). This macroRAFT was produced by chain extending PAA-TTC with PEGA, resulting in the reactivatable group being located at the end of the PPEGA block. In such a configuration, chain extension of the hydrophobic

monomers occurs from the PPEGA segments, leaving the PAA segment free to extend in water and be more effective as a stabilizing block, as shown in Fig. 2A and B. In addition, while the linear macroRAFT block copolymer, M2, contained 45 units of ethylene glycol (EG) (in a proportion slightly above stoichiometry to the number of AA units), M3 contains 36 EG units, resulting in an excess of AA units, which should increase stability. Finally, a greater amount of this macroRAFT is adsorbed on the surface of the clay at the concentration of macroRAFT selected (around 12 mol% of the total amount), as compared to M2, which is also desirable in order to promote the formation of hybrid morphologies.

The synthesis of hybrid latexes in the presence of M3 was carried out at three different pH values (3.0, 7.5 and 12) and stable latexes were obtained in all experiments, even under acidic conditions, confirming that a slight excess of AA units helped stabilization. The pending configuration of the PEG chains may have also eventually hindered the complexation between the PAA and the PPEGA blocks. An effect of the pH on particle size and particle size distribution could be, however, observed, as shown in Fig. S3 (ESI†). While one population of small particles of 76 nm was obtained when polymerization was carried out at pH 7.5, the presence of two populations of particles (Fig. S4, ESI†) at pH 3.0, which was the natural pH of the polymerization medium, resulted in high PdI values. This result might indicate that, in an acidic medium, particle aggregation can still occur in spite of the AA-rich stoichiometry of M3, likely due to the formation of some hydrogen bonds (AA/EO interactions), preventing the PAA block to fully stabilize the particles. The kinetic behavior of the synthesis was also affected by the pH (Fig. S3†). The lowest conversion (66%) was obtained at low pH (3.0), while a conversion of 98% was obtained at pH 7.5.

The hybrid latex synthesized at pH 7.5 (M3B) was characterized by cryo-TEM and the images are shown in Fig. 2C (see
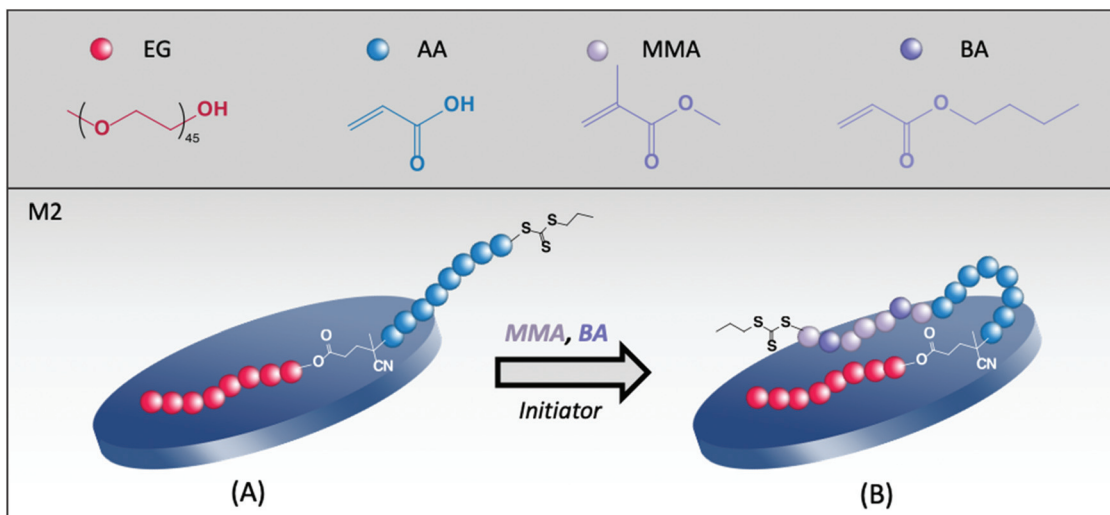

Fig. 1 Schematic representation of Laponite® platelets (A) with the adsorbed macroRAFT agent PEG$_{45}$-b-PAA$_{42}$-TTC (M2) and (B) during the synthesis of P(MMA-*co*-BA)/Laponite® nanocomposite latexes by RAFT-mediated surfactant-free emulsion polymerization using M2.

Fig. 2 Schematic representation of Laponite® platelets (A) with the adsorbed macroRAFT agent $PAA_{40}-b-PPEGA_4-TTC$ (M3) and (B) during the synthesis of P(MMA-co-BA)/Laponite® nanocomposite latexes by RAFT-mediated surfactant-free emulsion polymerization using M3. (C) The cryo-TEM images of hybrid particles obtained by the copolymerization of MMA : BA 80 : 20, at 80 °C, in the presence of 2.2 mM of the macroRAFT agent M3 and 5 g L^{-1} of Laponite® at pH 7.5 (R3B).

also Fig. S10 in the ESI†). Statistical analysis of a large number of particles indicated the formation of small nodules of *ca.* 31 nm in diameter, in agreement with the formation of self-assembled block copolymers (Fig. S9A, ESI†). No conclusion can be drawn, however, regarding the effective number of composite particles because, to be identified, the clay platelets must have their basal planes oriented in parallel to the electron beam, whereas in cryo-TEM, the platelets are trapped inside frozen water and are therefore randomly oriented. In addition, if the basal plane of a platelet is perpendicular to the electron beam, hybrid particles could be erroneously detected as pure polymer particles. Still, polymeric nodules can be seen growing on top of inorganic particles, generating mainly Janus structures with one clay platelet on one side and a polymer

nodule on the other. Some dumbbell-shaped particles with one clay platelet sandwiched between two polymer nodes could also be occasionally seen. According to the adsorption isotherm of this macroRAFT,[24] about 12 mol% of the macroRAFT agent is adsorbed onto the Laponite® surface, while 88% is free in the aqueous phase before polymerization.

It is worth mentioning that, in REEP, part of the macroRAFT agent should be free in solution (non-adsorbed) and available to stabilize the growing composite particles. So usually an excess of macroRAFT is necessary, but if the excess is too large, it may lead to secondary nucleation and colloidal instability, as shown above for PAA-TTC. Although it should be ideally avoided, the presence of a certain amount of free polymer particles is, however, not necessarily an issue for the

formation of composite films, and if necessary, could be easily minimized by increasing the inorganic concentration. An estimation of the percentage of free polymer particles can be performed by comparing the number of Laponite® platelets present in the medium (based on their average dimensions and density[35]) with the number of nucleated polymer particles, as reported in the Experimental section. This calculation assumes that there are no free clay platelets (we indeed did not identify in the TEM images any black sticks which would correspond to the Laponite® clay), and that all composite particles have a Janus morphology (*i.e.*, the number of composite nodules is equal to the number of clay platelets). For R3B, the estimation of the fraction of free polymer particles according to this method is ~16%. Considering that a small fraction of the clay platelets is also surrounded by two polymer nodes, forming dumbbell-shaped particles, such calculation actually overestimates the amount of free latex particles, but was nevertheless considered to provide a useful basis for discussion.

3.4. Hybrid latexes synthesized with PAA_{40}-*b*-$P(PEGA_6$-*co*-$BA_4)$ (M4)

To decrease the hydrophilicity of the macroRAFT agent and thus favor its adsorption onto Laponite® platelets, a more hydrophobic block copolymer containing BA units along the P(PEGA) block, PAA_{40}-*b*-$P(PEGA_6$-*co*-$BA_4)$-TTC (M4, Table 1), was designed and evaluated. According to the adsorption isotherm of this macroRAFT,[24] about 15 mol% of the macroRAFT agent is adsorbed onto the Laponite® surface, while 85% is free in the aqueous phase prior to polymerization. However, besides contributing to decrease the macroRAFT agents' predisposition to stay preferentially in the aqueous phase, the BA units also increase the affinity of the hydrophobic monomers for the clay platelets' environment, encouraging the polymerization to take place at their surface, as shown in Fig. 3A and B.

Stable latexes were obtained for all three different pH values tested (5.0, 7.5 and 12). As this macroRAFT is more hydrophobic than M3, the lowest pH tested had to be

Fig. 3 Schematic representation of Laponite® platelets (A) with the adsorbed macroRAFT agent PAA_{40}-*b*-$P(PEGA_6$-*co*-$BA_4)$-TTC (M4) and (B) during the synthesis of P(MMA-*co*-BA)/Laponite® nanocomposite latexes by RAFT-mediated surfactant-free emulsion polymerization using M4. (C) The cryo-TEM images of hybrid particles obtained by the copolymerization of MMA : BA 80 : 20, at 80 °C, in the presence of 2.2 mM of M4 and 5 g L^{-1} of Laponite® at pH 7.5 (R4B).

increased as compared to M3 due to solubility issues. Again, the pH seemed to affect conversion, since the highest instantaneous and overall conversions were obtained at neutral pH (Fig. S5A†). The hybrid latex synthesized at pH 7.5 (R4B) was characterized by cryo-TEM and the images are shown in Fig. 3C. It is again possible to identify Janus particles but, more remarkably when compared to R3B, dumbbell and multipod particles (multiple polymer nodules per clay), depending on the size of the clay platelets. The number average diameter of the nodules, determined by statistical analysis of the cryo-TEM images, was 24 nm, slightly smaller than for R3B (31 nm). When considering that all particles have a Janus morphology, the percentage of free polymer nodules can be estimated as being 62%. However, due to the considerable amount of dumbbell particles formed, the actual value is presumably much lower. Indeed, as seen in Fig. 3C, the presence of BA units increased the interaction with the clay platelets and helped confining the polymerization on both faces of the clay platelets, favoring the production of a dumbbell morphology. In addition, as the polymer grew on both sides, and was therefore distributed over a larger surface area, it is coherent that smaller nodules were formed in this case as compared to R3B. With the assumption that all composite particles have a dumbbell shape, the fraction of free polymer particles reduced to 23%.

Interestingly, there seems to be no direct correlation between the amount of free macroRAFT agent and the proportion of free polymer nodules. Indeed, in both cases (M3 and M4), a large amount of free macroRAFT was present at the beginning of polymerization, which was not reflected in the final number of free latex particles that were proportionally less abundant. Although this would require further investigation, such observation would indicate that the free macroRAFT, in these cases, was less engaged in the formation of free latex particles and more in the stabilization of the hybrid particles. And, for this reason, the control over the affinity of the macroRAFT for Laponite® is essential, as it will determine which of these two mechanisms predominates.

However, recent studies have demonstrated that the final morphology of clay-based nanocomposite particles is the result of the interplay between not only kinetic but also thermodynamic factors.[21,36,37] Clays, for being very hydrophilic, tend to minimize contact with the (hydrophobic) polymeric phase by maintaining themselves in a state of minimal interfacial energy. So, depending on the glass transition temperature (T_g) of the polymer matrix (and therefore on the mobility that the inorganic phase has in it), the inorganic nanoparticle can exclude itself from inside the hydrophobic polymer phase, searching for the polymer/water interface and generating Janus or armored morphologies. In this respect, the selection of an adequate ratio between the comonomers MMA and BA must consider the T_g of the final copolymer. Using the Fox equation,[38] the approximate T_g of the monomer composition used in the previous polymerizations (MMA : BA 80 : 20 in weight) is 58 °C ($T_{g, BA} = -54$ °C and $T_{g, PMMA} = 106$ °C). To prevent the inorganic particles from excluding

themselves from the polymer phase, and guarantee kinetically controlled morphology, the T_g of the copolymer should be superior to the temperature used during the synthesis of the nanocomposite latex particles. The use of an MMA-richer feeding might be necessary, in this case, to increase the T_g of the final copolymer and guarantee the formation of core–shell hybrid latex particles. Hence, two additional experiments (under the same conditions as R4B) were carried out to evaluate the effect of different MMA : BA mixtures by increasing the MMA molar ratio from 80% to 90% (R4D, MMA : BA 90 : 10, $T_{g, FOX} = 80$ °C) and to 100% (R4E, $T_g = 106$ °C). The results of the evolution of overall and instantaneous conversion with time, as well as the evolution of particle size and PdI values with conversion, are shown and discussed in the ESI (Fig. S6A and B,† respectively). They indicate that the polymerization of pure MMA (R4E) presented an induction period and lower instantaneous conversions (ESI†). Indeed, these results confirm that chain extension takes more time for pure MMA than for MMA/BA copolymers, as BA helps the fragmentation to occur more efficiently.[39] In addition, low instantaneous conversion is known to cause the formation of droplets of the accumulated monomer that can compete for the adsorption of macroRAFT stabilizers and Laponite® platelets, and act as plasticizers, decreasing the T_g of the polymer shell, which is undesirable in the current strategy. It can be considered that R4D, on the other hand, presented no changes on the morphology in comparison to R4B, as seen from similar kinetic and particle size profiles, and so, for precaution, the following experiments R5 and R6 were carried out with the monomer mixture MMA : BA 90 : 10.

3.5. Hybrid latexes synthesized with P(PEGA$_5$-co-BA$_3$) (M5)

A non-ionic macroRAFT agent, P(PEGA$_5$-co-BA$_3$)-TTC (M5, Table 1), was next evaluated in the synthesis of nanocomposite particles by emulsion polymerization. Since this macroRAFT does not contain AA units, the pH of the macroRAFT/Laponite® suspension (pH = 10) was not adjusted prior to the emulsion polymerization and a peptizer was added to neutralize the rim charges of Laponite®. However, the first experiment (R5A) resulted in an unstable final latex, probably due to the absence of the PAA block. To increase the colloidal stability of the hybrid particles, the experiment was repeated by submitting the colloidal suspension of this macroRAFT agent and Laponite® to 5 minutes of sonication at 30% amplitude before polymerization (R5B) resulting in a stable latex with a final DLS particle size of 132 nm (Fig. S7B, ESI†). To verify the stability of the particles in the absence of Laponite® platelets, a blank experiment without Laponite® was also carried out at the same pH (R5C).

The presence of Laponite® resulted in an increase in instantaneous and overall final conversions (Fig. S7A, ESI†). It is interesting to note that conversion reached a plateau at ~80% in the presence of Laponite® and at ~70% in the absence of the clay. As this macroRAFT agent is not pH-sensitive, the high pH of the medium is not expected to affect chain extension in this case. It is likely therefore that stability issues

caused the limiting conversion. From the evolution of particle size and PdI (Fig. S7B†), it is indeed possible to confirm that this non-ionic macroRAFT does not behave as an efficient stabilizer for the pure polymer particles, similarly to what has already been described in the literature for PEG-TTC.[40] Considering that instantaneous conversion was not 100% (and was particularly low in the absence of clay), the stability issue may be related to the fact that this macroRAFT agent can partition between the monomer and water phases in the course of polymerization, which would lead to a diminution of the amount of macroRAFT effectively available to stabilize the forming particles.

The cryo-TEM images of the stable part of latex R5A, shown in Fig. 4, reveal again a tendency of the platelets to be located at the edges of the polymeric particles, forming Janus structures, or sandwiched between two polymer particles, in the so-called dumbbell morphology. A few armored particles with two or three platelets surrounding the polymer particles can also be seen. In addition, the largest particles appear to be non-spherical, which can be an indication of limited colloidal stability, confirming that this macroRAFT agent is not a very efficient stabilizer.

In a recent work,[22] similar results were obtained for MMT, using a similar macroRAFT agent. In the case of MMT, however, the instability of the system was overcome with the addition of an anionic copolymer that acted in conjunction with the non-ionic macroRAFT to guarantee colloidal stability. This strategy led to a good wettability of MMT basal faces, leading to an almost full coverage of the clay. Finally, it is worth pointing out that this macroRAFT has not been able to assist the encapsulation of Laponite® platelets, although it was successful for the encapsulation of silica.[16] This difference in behavior highlights the determinant role of the nature and surface chemistry of the inorganic particles. As the macroRAFT adsorbs more on the faces than on the edges of the clay, it leaves the edges, which are more energetic than the faces, uncovered. Therefore, this macroRAFT agent can be considered quite sensitive to different morphologies and/or surface chemistry. Particularly in the case of Laponite®, in which the opposite charges on the surface and on the edges, surface energy and high aspect ratio of the platelets play an important role. So, for an efficient encapsulation of clay platelets while maintaining a good colloidal stability, it might be necessary to resort to other strategies, such as the association of M5 with another macroRAFT agent, for instance.

3.6. Hybrid latexes synthesized with P(AA$_{16}$-co-BA$_{16}$) (M6)

Several works have reported the successful encapsulation of various inorganic particles using P(AA-co-BA) RAFT copolymers or oligomers, with different compositions and molar masses.[5,10,11,17,20] In fact, in all cases, these macroRAFTs presented a high affinity with the oppositely charged inorganic surface, and were therefore capable of adsorbing onto the particles *via* a strong electrostatic interaction. In the case of Laponite®, on the other hand, this macroRAFT has been shown to adsorb onto the clay mainly by a hydrophobic interaction as the AA units are not expected to promote adsorption.[24] Interestingly enough, the adsorbed amount of P(AA$_{16}$-co-BA$_{16}$)-TTC (M6, Table 1) (320 mg g^{-1}) on Laponite® was close to the adsorbed amount of PAA$_{40}$-b-PPEGA$_4$ (M3, 453 mg g^{-1}), although in M6 the AA units were not grouped in block and M6 also does not contain PEGA units. Both characteristics would favor adsorption, which confirms the influence of the BA units in adsorption. Nevertheless, emulsion polymerization mediated by P(AA$_{16}$-co-BA$_{16}$)-TTC (M6, Table 1), with 13 mol% of the macroRAFT initially adsorbed onto Laponite®,[24] was carried out at pH 7.5 (R6). A stable latex was obtained and, from the cryo-TEM micrographs of Fig. 5 (see also Fig. S11 in

Fig. 4 The cryo-TEM images of hybrid particles obtained by the copolymerization of MMA : BA 90 : 10, at 80 °C, in the presence of 2.2 mM of the macroRAFT agent P(PEGA$_5$-co-BA$_3$)-TTC (M5) and 5 g L^{-1} of Laponite® at pH 10 (R5B).

Fig. 5 The cryo-TEM images of hybrid particles obtained by the copolymerization of MMA : BA 90 : 10, at 80 °C, in the presence of 2.2 mM of the macroRAFT agent P(AA$_{16}$-co-BA$_{16}$)-TTC (M6) and 5 g L^{-1} of Laponite® at pH 7.5 (R6).

the ESI†), it is possible to infer that this macroRAFT agent is capable of minimizing the surface energy difference between Laponite® and polymer, resulting in a better wetting of the inorganic surface than the previous macroRAFT agents, which is quite unexpected considering that M6 adsorbs less on Laponite® than M5.[24] As a result, a few non-spherical flat structures (flat Janus and sandwich or macaron-shaped particles), in which inorganic particles are better wetted by the polymer phase, were produced.

This result can be related to the interfacial properties of the platelets. Indeed, the surface energy of the edges can be considered higher than the surface energy of the basal faces and, therefore, the polymer phase still does not cover the edge surface. However, the presence of BA units favored adsorption due to hydrophobic interactions between these moieties in the macroRAFT agent chains and the clay basal surface. This, in turn, resulted in a decrease in the interfacial energy between the polymer and inorganic phases, enabling the polymer to better spread on the surface, while the AA units may have stayed away from the surface promoting stability. On the other hand, even though the adsorbed amount of M5 was higher, this macroRAFT agent contains hydrophilic PEGA units that can adsorb on the clay surface, thus increasing polymer/clay interfacial tension in comparison to M6 that is more hydrophobic, resulting in the formation of phase-separated spherical nodules.

From the above observations, we demonstrate that two competing processes can influence the stability and morphology of the nanocomposite latexes depending on (i) the fraction of the free macroRAFT agent and (ii) its ability to more or less efficiently direct the polymerization to the surface of the clay. According to this, two scenarios are possible: (i) pure instability: the fraction of free macroRAFT is so large that it drives polymerization to outside the clay environment and directs it

to the water phase, which is detrimental to stability; (ii) morphology control: if enough macroRAFT is adsorbed on the clay, polymerization is shifted more efficiently to the Laponite® surface. In the first case, the composition of the chains and the pH play a crucial role, while, in the second case, the surface energy of the platelets is of major importance. In this respect, the presence of BA units on the macroRAFT structure (as an alternative to PEG) can be an interesting strategy for tuning the morphology of the hybrid particles. However, all phenomena are strictly connected and interdependent, and so the final morphology will be the result of this interplay between different factors such as the fraction of free macroRAFT, the wettability of the clay surface and the conformation adopted by the chains.

4. Conclusions

We studied the effect of the nature of macroRAFT agents on the stability and morphology of Laponite®-containing nanocomposite latexes prepared via the REEP strategy. Due to the high hydrophilicity of PAA and the limited adsorption of this macroRAFT agent onto Laponite®, a large quantity of PAA was present in water prior to the polymerization. Consequently, the formation of secondary particles was promoted, leading to stability issues. The incorporation of PEG (linear, PEG$_{45}$-b-PAA$_{42}$, or pendent, PAA$_{40}$-b-PPEGA$_4$, chains) into the PAA block favored the approach of PAA to the clay basal surface, resulting mostly in the formation of Janus particles. So, instead of favoring the formation of free polymer particles, formed according to the PISA mechanism, the non-adsorbed fraction of this double hydrophilic macroRAFT agent was mainly devoted to the stabilization of the hybrid particles. The incorporation of BA units in PAA$_{40}$-b-P(PEGA$_6$-co-BA$_4$) to yield a more hydro-

phobic macroRAFT agent resulted in higher copolymer adsorption, promoting the formation of dumbbell particles as polymer growth took place on both faces of the Laponite® platelets. The absence of AA units in P(PEGA-co-BA) decreased the tendency of such macroRAFT to stay in the aqueous phase but resulted in limited colloidal stability due to its higher hydrophobicity. Finally, better wetting of the clay surface was attained with P(AA-co-BA) macroRAFT. Although this copolymer adsorbed less on Laponite® than the PEG-based macroRAFT agents, disposing of BA instead of PEGA minimized the surface energy of the clay and, the basal surface being relatively more hydrophobic, the polymer could better wet the surface and spread, resulting in particles with a flat morphology.

We have shown here the versatility of the REEP process to generate Laponite®-containing nanocomposite particles with controlled morphology. Yet Janus and dumbbell morphologies were predominantly observed, with the polymerization taking place on the clay faces and the edges remaining polymer-free. The use of cationic RAFT copolymers seems to be an interesting alternative to extend the approach to other morphologies as these copolymers would interact strongly with the Laponite® basal surface and further shift the polymerization locus to the Laponite® surface. This and the preparation of film-forming Laponite®-containing hybrid latexes are the subject of an ongoing work.

Conflicts of interest

There are no conflicts to declare.

Acknowledgements

References

1 J. A. Balmer, A. Schmid and S. P. Armes, *J. Mater. Chem.*, 2008, **18**, 5722–5730.

2 V. Mittal, in *Polymer Nanocomposites by Emulsion and Suspension Polymerization*, The Royal Society of Chemistry, 2011, pp. 1–31, DOI: 10.1039/9781849732192-00001.

3 V. Prevot and E. Bourgeat-Lami, in *Layered Double Hydroxide Polymer Nanocomposites*, ed. S. Thomas and S. Daniel, Woodhead Publishing, 2020, pp. 461–495, DOI: 10.1016/B978-0-08-101903-0.00011-8.

4 F. Dalmas, S. Pearson, B. Gary, J.-M. Chenal, E. Bourgeat-Lami, V. Prévot and L. Chazeau, *Polym. Chem.*, 2018, **9**, 2590–2600.

5 D. Nguyen, H. S. Zondanos, J. M. Farrugia, A. K. Serelis, C. H. Such and B. S. Hawkett, *Langmuir*, 2008, **24**, 2140–2150.

6 P. B. Zetterlund, S. C. Thickett, S. Perrier, E. Bourgeat-Lami and M. Lansalot, *Chem. Rev.*, 2015, **115**, 9745–9800.

7 E. Bourgeat-Lami, F. D'Agosto and M. Lansalot, in *Controlled Radical Polymerization at and from Solid Surfaces*, ed. P. Vana, Springer International Publishing, Heidelberg, 2016, vol. 270, pp. 123–161.

8 J.-C. Daigle and J. P. Claverie, *J. Nanomater.*, 2008, **2008**, 1–8.

9 P. Das, W. Zhong and J. P. Claverie, *Colloid Polym. Sci.*, 2011, **289**, 1519–1533.

10 P. Das and J. P. Claverie, *J. Polym. Sci., Part A: Polym. Chem.*, 2012, **50**, 2802–2808.

11 N. Zgheib, J.-L. Putaux, A. Thill, E. Bourgeat-Lami, F. D'Agosto and M. Lansalot, *Polym. Chem.*, 2013, **4**, 607–614.

12 J. Garnier, J. Warnant, P. Lacroix-Desmazes, P. E. Dufils, J. Vinas, Y. Vanderveken and A. M. van Herk, *Macromol. Rapid Commun.*, 2012, **33**, 1388–1392.

13 J. Garnier, J. Warnant, P. Lacroix-Desmazes, P.-E. Dufils, J. Vinas and A. van Herk, *J. Colloid Interface Sci.*, 2013, **407**, 273–281.

14 J. Warnant, J. Garnier, A. van Herk, P.-E. Dufils, J. Vinas and P. Lacroix-Desmazes, *Polym. Chem.*, 2013, **4**, 5656–5663.

15 K. Li, P.-Y. Dugas, E. Bourgeat-Lami and M. Lansalot, *Polymer*, 2016, **106**, 249–260.

16 E. Bourgeat-Lami, A. J. P. G. França, T. C. Chaparro, R. D. Silva, P. Y. Dugas, G. M. Alves and A. M. Santos, *Macromolecules*, 2016, **49**, 4431–4440.

17 S. I. Ali, J. P. A. Heuts, B. S. Hawkett and A. M. van Herk, *Langmuir*, 2009, **25**, 10523–10533.

18 V. T. Huynh, D. Nguyen, C. H. Such and B. S. Hawkett, *J. Polym. Sci., Part A: Polym. Chem.*, 2015, **53**, 1413–1421.

19 A. C. Perreira, S. Pearson, D. Kostadinova, F. Leroux, F. D'Agosto, M. Lansalot, E. Bourgeat-Lami and V. Prévot, *Polym. Chem.*, 2017, **8**, 1233–1243.

20 S. Pearson, M. Pavlovic, T. Augé, V. Torregrossa, I. Szilagyi, F. D'Agosto, M. Lansalot, E. Bourgeat-Lami and V. Prévot, *Macromolecules*, 2018, **51**, 3953–3966.

21 M. A. Mballa Mballa, S. I. Ali, J. P. A. Heuts and A. M. van Herk, *Polym. Int.*, 2012, **61**, 861–865.

22 R. D. Silva, T. D. C. Chaparro, I. S. Monteiro, P.-Y. Dugas, F. D'Agosto, M. Lansalot, A. Martins dos Santos and E. 'Bourgeat-Lami, *Macromolecules*, 2019, **52**, 4979–4988.

23 T. R. Guimaraes, T. D. C. Chaparro, F. D'Agosto, M. Lansalot, A. M. dos Santos and E. Bourgeat-Lami, *Polym. Chem.*, 2014, **5**, 6611–6622.

24 T. D. C. Chaparro, R. D. Silva, I. S. Monteiro, A. Barros-Timmons, R. Giudici, A. Martins dos Santos and E. Bourgeat-Lami, *Langmuir*, 2019, **35**, 11512–11523.

25 Y. Liu, M. F. Zhu, X. L. Liu, W. Zhang, B. Sun, Y. M. Chen and H. J. P. Adler, *Polymer*, 2006, **47**, 1–5.

26 M. Dijkstra, J. P. Hansen and P. A. Madden, *Phys. Rev. Lett.*, 1995, **75**, 2236–2239.

27 H. Mori, A. H. E. Müller and J. E. Klee, *J. Am. Chem. Soc.*, 2003, **125**, 3712–3713.

28 F. A. Plamper, H. Becker, M. Lanzendörfer, M. Patel, A. Wittemann, M. Ballauff and A. H. E. Müller, *Macromol. Chem. Phys.*, 2005, **206**, 1813–1825.

29 I. Chaduc, A. Crepet, O. Boyron, B. Charleux, F. D'Agosto and M. Lansalot, *Macromolecules*, 2013, **46**, 6013–6023.

30 R. L. Parfitt and D. J. Greenland, *Clay Miner.*, 1970, **8**, 305–315.

31 X. G. Qiao, P. Y. Dugas, B. Charleux, M. Lansalot and E. Bourgeat-Lami, *Polym. Chem.*, 2017, **8**, 4014–4029.

32 W. Zhang, F. D'Agosto, O. Boyron, J. Rieger and B. Charleux, *Macromolecules*, 2012, **45**, 4075–4084.

33 Č. Koňák and M. Sedlák, *Macromol. Chem. Phys.*, 2007, **208**, 1893–1899.

34 S. Holappa, L. Kantonen, F. M. Winnik and H. Tenhu, *Macromolecules*, 2004, **37**, 7008–7018.

35 H. Z. Cummins, *J. Non-Cryst. Solids*, 2007, **353**, 3891–3905.

36 M. A. M. Mballa, J. P. A. Heuts and A. M. van Herk, *Colloid Polym. Sci.*, 2013, **291**, 501–513.

37 A. M. van Herk, *Macromol. React. Eng.*, 2016, **10**, 22–28.

38 T. G. Fox, *Bull. Am. Phys. Soc.*, 1956, **1**, 123.

39 J. B. McLeary, F. M. Calitz, J. M. McKenzie, M. P. Tonge, R. D. Sanderson and B. Klumperman, *Macromolecules*, 2005, **38**, 3151–3161.

40 T. Rodrigues Guimaraes, T. de Camargo Chaparro, F. D'Agosto, M. Lansalot, A. Martins Dos Santos and E. Bourgeat-Lami, *Polym. Chem.*, 2014, **5**, 6611–6622.